Research Article   Open Access

Gene Expression Profiling and Bioinformatic Analysis of Rabbit Basilar Artery after Experimental Subarachnoid Hemorrhage

Satoshi Matsuo, Yuichiro Kikkawa*, **Masaaki Hokama, Ryota Kurogi, Akira Nakamizo, Masahiro Mizoguchi and Tomio Sasaki**

Department of Neurosurgery, Graduate School of Medical Sciences, Kyushu University, 3-1-1 Maidashi, Higashi-ku, Fukuoka 812-8582, Japan

*Corresponding author: Yuichiro Kikkawa, Department of Neurosurgery, Graduate School of Medical Sciences, Kyushu University, 3-1-1 Maidashi, Higashi-ku, Fukuoka 812-8582, Japan, Tel: +81-92-642-5524; Fax: +81-92-642-5526; E-mail: ykikkawa@ns.med.kyushu-u.ac.jp

Abstract

Objective: The molecular mechanisms which contribute to the development of vascular events including cerebral vasospasm after subarachnoid hemorrhage (SAH) in cerebral artery remain to be elucidated. In this study, we investigated the time course of changes in the gene expression of cerebral artery using rabbit SAH model and performed bioinformatic analysis of differentially expressed genes.

Methods: Rabbit basilar arteries were harvested on days 3, 5, and 7 after initial hemorrhage. Changes in gene expression of the rabbit basilar artery were investigated by using Agilent rabbit oligo microarrays and analyzed the data by Ingenuity Pathway Analysis (IPA).

Results: Among investigated 43,623 genes, 1,121 genes were differentially expressed at least 1 time point. We found that the number, magnitude of fold change, and gene expression pattern were most dynamically changed on day 3, whereas narrowing of the basilar artery became most severe on day 5. In microarray datasets analyzed by IPA revealed that 25 biological functions identified from differentially expressed genes were significantly upregulated.

Conclusion: Our findings that were based on gene expression analysis followed by bioinformatic analysis may provide a simple basis to interlink the various presumed pathogenesis of vascular events including cerebral vasospasm after SAH.

Introduction

Cerebral vasospasm is one of the most important cerebrovascular events following SAH and characterized by delayed and prolonged contraction of cerebral arteries, which may cause cerebral ischemia and lead to death or neurological deficits in patients with SAH [1]. Therefore, the prevention and treatment of vasospasm have an important role in the management of SAH patients. However, molecular mechanisms, including alterations in gene expression and functional changes in cerebral arteries after SAH that contribute to the development of cerebral vasospasm, remain to be elucidated.

The gene microarray method allows simultaneous analysis of the expression of thousands of genes. This technology promises to allow investigation of the entire genome on a single chip so that researchers can obtain a global picture of the interactions among thousands of genes simultaneously. This technique will also provide insight into the underlying mechanisms of many diseases. In some diseases, such as myocardial infarction and intracranial aneurysm, microarrays have been used to elucidate pathological mechanisms by identifying pathogenic genes and their interaction in networks [2-4].

Cerebral vasospasm is thought to be a biologically complex and multifactorial pathological condition. Therefore, this new approach will produce a broad view of the pathological mechanisms by identifying pathogenic genes and their interaction in various functional networks. Moreover, analyzing chronological changes in gene expression of cerebral artery may be helpful for elucidating the mechanism of cerebral vasospasm because the delayed onset is a fundamental feature of the pathophysiology of cerebral vasospasm.

In this study, we used microarray analysis to investigate chronological changes in gene expression in the basilar artery in the rabbit SAH model. Moreover, to elucidate how differentially expressed genes (DEGs) interact during the development of cerebral vasospasm, Ingenuity Pathway Analysis (IPA, Ingenuity Systems, and Redwood City, CA, USA) was performed.

Materials and Methods

Preparation of the rabbit SAH model

This study was conducted in accordance with the guidelines for proper conduct of animal experiments published by the Science Council of Japan. The study protocol was approved by the Animal Care and Use Committee, Kyushu University (Permit Number: A24-103-0). Adult male Japanese white rabbits (2.5 to 3.0 kg) were anesthetized with an intramuscular injection of ketamine (40 mg/kg weight) and an intravenous injection of sodium pentobarbital (20 mg/kg weight). On day 0, 0.5 ml cerebrospinal fluid was aspirated percutaneously from the cisterna magna using a 23-gauge-butterfly

needle, and then 2.5 ml of non-heparinized autologous arterial blood obtained from the central ear artery was injected over 1 minute. The animal was kept in a prone position with the head tilted down at 30° for 30 minutes. During the animal preparation, blood clot formation was not observed in the syringe. On day 2, a second injection of autologous blood was similarly performed. The rabbits which were not subjected to SAH were used as controls (day 0).

Harvest of rabbit basilar arteries

On days 3 (n = 3), 5 (n = 3), and 7 (n = 3) after the first hemorrhage, the rabbits were heparinized (400 U/kg weight), euthanized by intravenous injection of an overdose of sodium pentobarbital (120 mg/kg weight), and exsanguinated from the common carotid artery. Exposing the brain revealed clot formation over the surface of the pons and the basilar artery in the SAH animals (Figure 1A). Immediately after excising the whole brain en bloc, subarachnoid membrane was carefully dissected and the clot was gently removed with micro-scissors and micro-forceps not to touch the basilar artery under a binocular microscope (Leica EZ4D, Leica Microsystems, Wetzler, Germany). Distal half of the surface of basilar artery was covered with thick clot in all rabbits with SAH (Figure 1A). Therefore, to estimate vasospasm, the external diameter of the basilar artery was measured at the point of the distal one-third of the rabbit basilar artery. The ventral surface of the whole brain was photographed with a digital camera (CX3, Richo, Tokyo, Japan) and the external diameter of the basilar artery was analyzed withImageJ (National Institute of Health, Bethesda, MD, USA). The entire length of basilar artery was then immediately excised from the brain and dissected free from surrounding tissues with micro-scissors and micro-forceps. Intraluminal blood was gently hand-flushed with normal physiological salt solution (123 mmol/L NaCl, 4.7 mmol/L KCl, 1.25 mmol/L $CaCl_2$, 1.2 mmol/L $MgCl_2$, 1.2 mmol/L KH2PO4, 15.5 mmol/L $NaHCO_3$, and 11.5 mmol/L D-glucose) using tuberculin syringe, and then the basilar artery was frozen in liquid nitrogen. The frozen tissues were stored at −80°C until use. Basilar arteries harvested from the rabbits which were not subjected to SAH were used as controls (day 0; n = 3).

Total RNA isolation from rabbit basilar arteries

Total RNA was extracted from the basilar arteries using TRIzol Reagent (Invitrogen, Carlsbad, CA, USA), according to the manufacturer's protocols. The quality of total RNA was evaluated with a spectrophotometer (Nano-Drop2000c; Thermoscientific, Wilmington, DE, USA) and gel electrophoresis (Experion; Bio-Rad, Hercules, CA, USA). RNA samples with an A260/280 ratio higher than 1.8 and with an RNA Quality Index higher than 9.0 was used for the gene expression microarray. Gene expression microarray analysis of rabbit basilar arteries

From 50 ng total RNA, cRNA was amplified, labeled, and hybridized to a Rabbit gene expression microarray (Agilent Technologies, Santa Clara, CA, USA) using the Low Input Quick Amp one-color Labeling kit (Agilent Technologies) according to the manufacturer's instructions. All hybridized microarray slides were scanned with an Agilent Microarray scanner G2505B (Agilent Technologies). Relative hybridization intensities and background hybridization values were calculated using Agilent Feature Extraction Software (9.5.1.1) (Agilent Technologies). Raw signal intensities and flags for each probe were calculated from hybridization intensities and spot information, as recommended by Agilent. The raw signal intensities of samples were log_2 transformed and normalized using a quantile algorithm with the 'preprocessCore' library package of Bioconductor software [5,6]. To compare the correlation of gene expression among samples at each time point, scatterplots were created, and the correlation coefficient was calculated using the statistical software R version 2.9.0 (http://cran.ism.ac.jp/). Then, we identified DEGs in the SAH model using the linear models for microarray analysis (limma) package of Bioconductor software [6,7]. Genes in SAH samples (days 3, 5 and 7) with a limma value of P<0.05 and an absolute limma log_2 fold-change ($|log_2$ fold change$|$) higher than 1.0 compared to the control samples (day 0) were defined as DEGs in this study. Signal intensities of DEGs were log_2 transformed, and hierarchical clustering by both samples and genes was performed and colored by distance from the median value using the Multi Experiment Viewer (MeV) version 4.8.0 (http://www.tm4.org/mev/) [8,9]. Microarray data are available from the Gene Expression Omnibus (GEO, http://www.ncbi.nlm.nih.gov/geo/) with the accession number GSE44910. In this study, we performed one microarray analysis per one rabbit because the amount of basilar artery from each rabbit is too small.
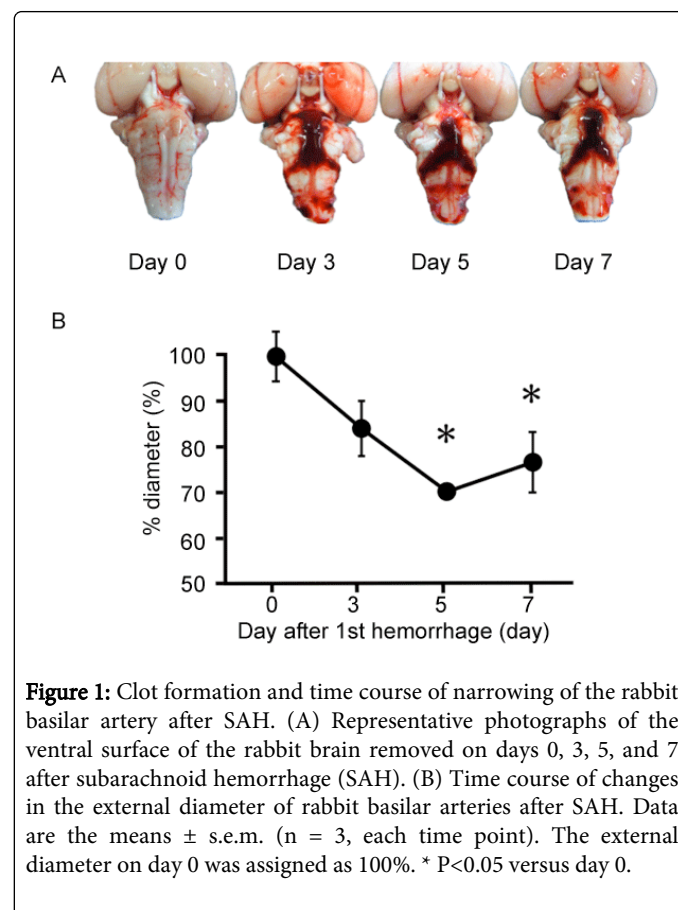

Figure 1: Clot formation and time course of narrowing of the rabbit basilar artery after SAH. (A) Representative photographs of the ventral surface of the rabbit brain removed on days 0, 3, 5, and 7 after subarachnoid hemorrhage (SAH). (B) Time course of changes in the external diameter of rabbit basilar arteries after SAH. Data are the means ± s.e.m. (n = 3, each time point). The external diameter on day 0 was assigned as 100%. * P<0.05 versus day 0.

Ingenuity Pathway Analysis (IPA)

We used a rabbit-specific microarray to investigate changes in levels of mRNA expression in the rabbit basilar arteries after SAH. Because limited genetic information is currently available for rabbits, the human orthologs of differentially expressed rabbit genes were retrieved from BioMart (http://www.biomart.org/) in the ensembl database and assigned to each rabbit probe. Bioinformatic analysis of

the DEGs was performed using IPA version 9.0 (Ingenuity Systems) with the Human Ensembl IDs as a query gene list.

The IPA identified biological functions that were most significant to the data set. DEGs that were associated with biological functions in the Ingenuity Knowledge Base (Ingenuity Systems) were used for the analysis. A right-tailed Fisher's exact test was used to calculate a p-value that determined the probability that each biological function assigned to that network or to the data set was due to chance alone.

Statistical analysis

The data are expressed as the mean value ± s.e.m. of the indicated experimental number. One basilar arterial preparation obtained from one animal was used for each experiment, and therefore the number of experiments (n value) also indicates the number of rabbits. Analysis of variance followed by Dunnett's post-hoc test was used to determine statistical difference in a multiple comparison with the control model (day 0). A value of $P < 0.05$ was considered to be statistically significant. All analyses were performed using GraphPad PRISM software version 5.0 (GraphPad Software, San Diego, CA, USA).

Results

Assessment of cerebral vasospasm following SAH

After SAH, blood clot formation was observed over the surface of the pons and the basilar artery in rabbits at each time point (Figure 1A). The external diameter of the basilar artery was $0.87 ± 0.048$ mm in the controls (day 0, n=3). On day 3, the basilar artery had narrowed to $83.9 ± 6.21\%$ of the control (n = 3). The narrowing reached a peak ($69.8 ± 0.10\%$ of the control) on day 5 (n = 3) and then gradually recovered to $76.4 ± 6.80\%$ of the control on day 7 (n = 3). The basilar artery was significantly narrowed on days 5 and 7 after SAH (Figure 1B).

Global gene expression in the rabbit basilar artery following SAH

To evaluate the reproducibility of the gene expression among the three rabbits at each time point, we performed scatterplot analysis of the gene expression. The graph showed that gene expression in the basilar artery of each rabbit was positively correlated among the three samples on each day (Figure 2). Correlation coefficients of samples were between 0.942 and 0.987. These strong positive correlation coefficients allowed us to perform subsequent gene expression analysis of the rabbit basilar artery after SAH.

Among investigated 43,623 genes, 1,121 genes were differentially expressed at least 1 time point. Eight hundred sixty-eight genes (1.99% of total gene probes) including 555 up regulated and 313 downregulated genes were differentially expressed on day 3. Six hundred three (1.38% of total gene probes) and 564 (1.29% of total gene probes) genes were differentially expressed on days 5 and 7, respectively (Table 1). To better visualize the temporal changes in the expression value of the DEGs following SAH, the number of DEGs at each time point was plotted against their corresponding $\log_2$ fold change (Figure 3). The gene expression data were represented as $\log_2$

fold change of SAH over day 0. This plot shows that 508 genes (91.5% of upregulated DEGson day 3), 404 genes (96.7% of upregulated DEGson day 5), and 357 genes (97.0% of upregulated DEGs on day 7) showed a $\log_2$ fold change between 1 and 3. Forty-seven genes (8.5% of upregulated DEGs on day 3), 14 genes (3.3% of upregulated DEGs on day 5), and 11 genes (3.0% of upregulated DEGs on day 7) were altered by a $\log_2$ fold change of more than 3. The number and magnitude of downregulated DEGs reached its peak on day 3 and decreased over time. Two hundred seventy-six genes (88.2% of downregulated DEG on day 3), 183 genes (98.9% of downregulated DEG on day 5), and 189 genes (96.4% of downregulated DEG on day 7) showed a $\log_2$ fold change between -1 and -2. Thirty-seven genes (11.8% of downregulated DEGs on day 3), 2 genes (1.1% of down-regulated DEGs on day 5), and 7 genes (3.6% of down-regulated DEGs on day 7) were altered by a $\log_2$ fold change of less than -2. As a result, the majority of up- and downregulated DEGs showed a $\log_2$ fold change between 1 and 3, and between -1 and -2, respectively. The number and magnitude of both up- and downregulated DEGs reached its peak on day 3 and decreased over time.
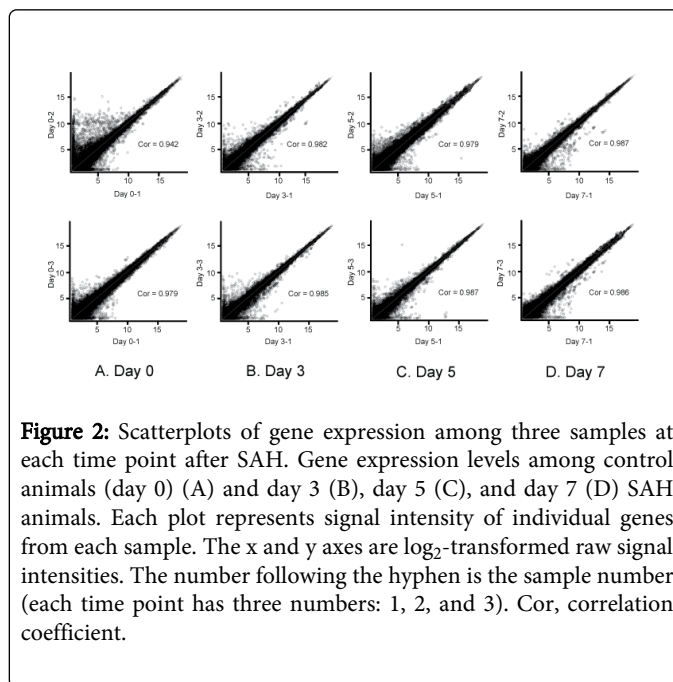

Figure 2: Scatterplots of gene expression among three samples at each time point after SAH. Gene expression levels among control animals (day 0) (A) and day 3 (B), day 5 (C), and day 7 (D) SAH animals. Each plot represents signal intensity of individual genes from each sample. The x and y axes are $\log_2$-transformed raw signal intensities. The number following the hyphen is the sample number (each time point has three numbers: 1, 2, and 3). Cor, correlation coefficient.

Day	The number of DEGs		
	Up regulated	Down regulated	Total (%)
3	555	313	868 (1.99)
5	418	185	603 (1.38)
7	368	196	564 (1.29)
The number of DEGs in each time point was listed.			

Table 1: The number of differentially expressed genes (DEGs) in the rabbit basilar artery after SAH.
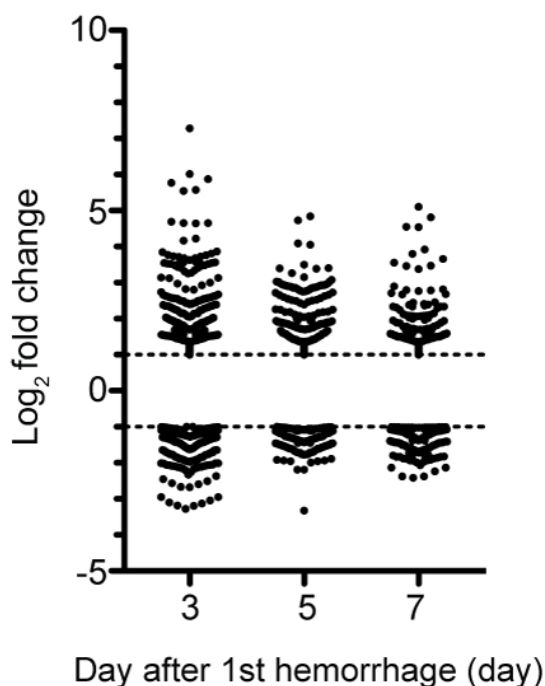
Figure 3: Scatter diagram of differentially expressed genes in the rabbit basilar artery after SAH. Plots in the scatter diagram showed individual up- and down-regulated genes on days 3, 5 and 7 compared to day 0. The broken lines indicated the threshold of $\log_2$ fold change. The upper broken line indicates $\log_2$ fold change = 1, and the lower one indicates $\log_2$ fold change = −1.

Hierarchical clustering of DEGs in the rabbit basilar artery

Next, hierarchical clustering was conducted on all DEGs (1,121 genes; 2.57% of all genes) to assess the similarity of the gene expression pattern in the basilar artery after SAH. A heat map was used to demonstrate the gene expression pattern of each sample (Figure 4). We observed a clear distinction in the gene expression pattern between SAH samples (days 3, 5, and 7) and control samples (day 0). According to the heat map, the gene expression pattern was dramatically changed between days 0 and 3. Among SAH animals, the gene expression patterns on days 5 and 7 were similar, according to the branch length.

Bioinformatic analysis of DEGs in the rabbit basilar artery after SAH

To better understand the biological roles of the DEGs in the basilar artery after SAH, we also performed a bioinformatic analysis of those genes. Using orthologous gene information, differentially expressed rabbit gene IDs were automatically converted human ensemble gene IDs. Then, the dataset of converted gene IDs was loaded into IPA, and bioinformatic analysis was performed. IPA categorized the 25 functional groupings from the uploaded datasets based on the Ingenuity Pathways Knowledge Base (Figure 5).
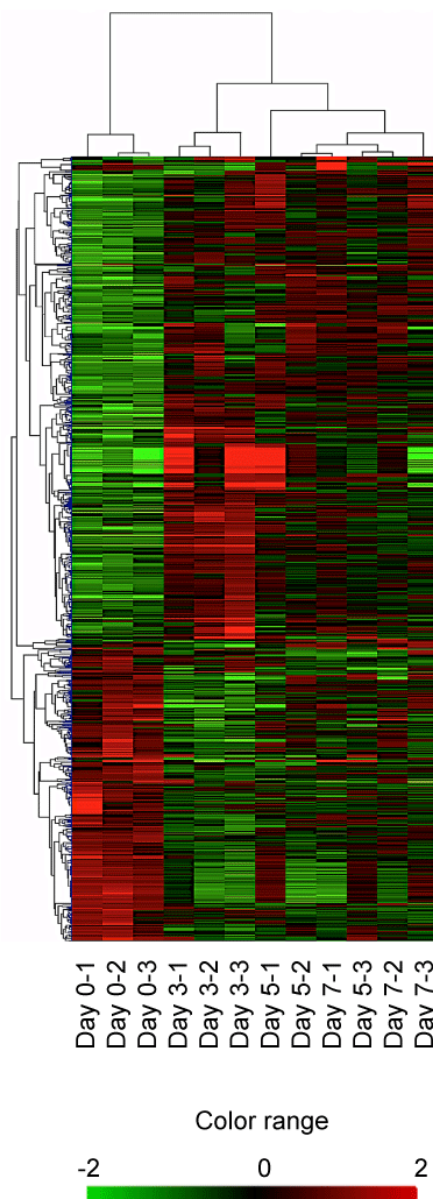

Figure 4: Clustering analysis of the differentially expressed genes in the rabbit basilar artery after SAH. Combined hierarchical clustering was applied to expression data of all differentially expressed genes (1,121 genes; 2.57% of all genes). Heat map representation of gene expression profiles. Each line across the map represents a single gene. Each column represents an array of genes (from day 0 to day 7). The number following the hyphen is the sample number (each time point has three numbers: 1, 2, and 3). Gene expression values were $\log_2$ transformed and median centered for each gene. The relative gene expression level is indicated by color and ranges from highly increased (intense red) to highly decreased (intense green), with black representing unchanged expression.
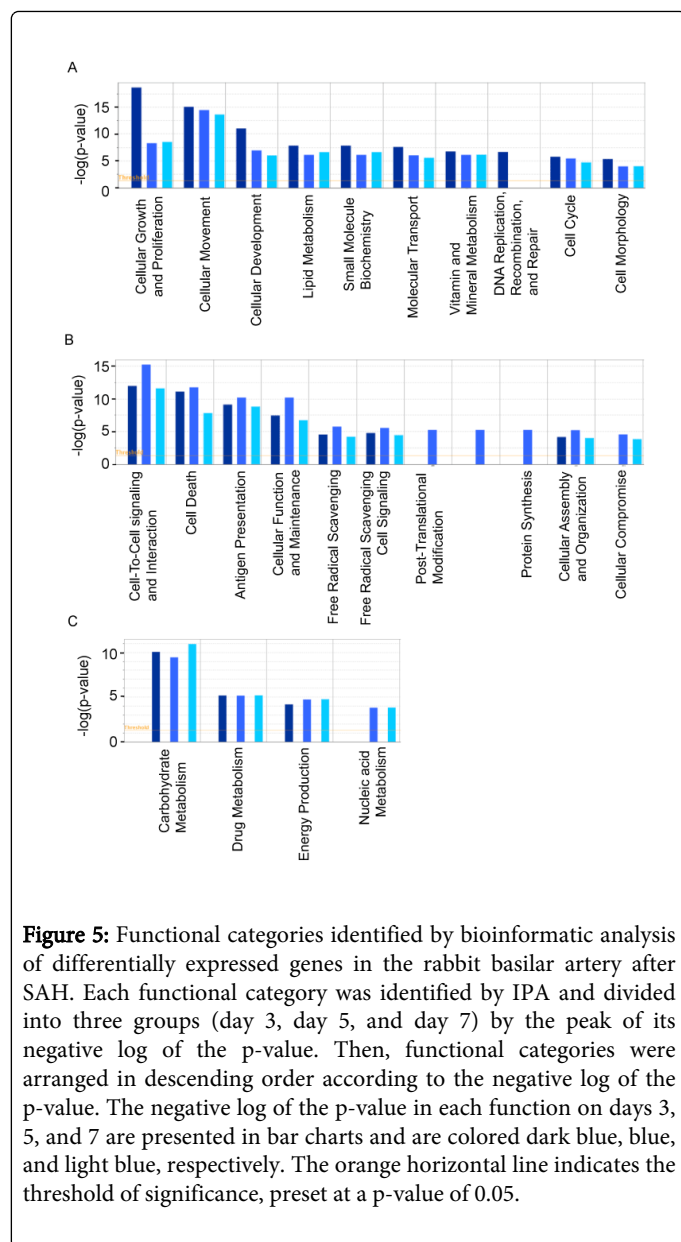
Figure 5: Functional categories identified by bioinformatic analysis of differentially expressed genes in the rabbit basilar artery after SAH. Each functional category was identified by IPA and divided into three groups (day 3, day 5, and day 7) by the peak of its negative log of the p-value. Then, functional categories were arranged in descending order according to the negative log of the p-value. The negative log of the p-value in each function on days 3, 5, and 7 are presented in bar charts and are colored dark blue, blue, and light blue, respectively. The orange horizontal line indicates the threshold of significance, preset at a p-value of 0.05.

A total of 10 biological functions including "cellular growth and proliferation", "cellular movement", "cellular development", "lipid metabolism", "small molecule biochemistry", "molecular transport", "vitamin and mineral metabolism", "DNA replication, recombination, and repair", "cell cycle" and "cell morphology" showed the highest significant peaks on day 3. A total of 11 biological functions including "cell-to-cell signaling and interaction", "cell death", "antigen presentation", "cellular function and maintenance", "free radical scavenging", "cell signaling", "post-translational modification", "protein degeneration", "protein synthesis", "cellular assembly and organization" and "cellular compromise" showed the highest significant peaks on day 5. The following four biological functions showed the highest significant peaks on day 7: "carbohydrate metabolism", "drug metabolism", "energy production" and "nucleic acid metabolism".

Moreover, IPA identified not only these functional categories but also downstream cellular functions and included genes (Supplementary Table 1).

Discussion

The present study demonstrated the chronological changes in gene expression in the rabbit basilar artery after SAH using microarray analysis. Furthermore, chronological changes in the gene ontology-based functional classification of DEGs were demonstrated by analyzing microarray datasets with IPA.

We investigated the correlation between chronological changes in gene expression and the time course of the development of cerebral vasospasm in the rabbit basilar artery at four time points (0, 3, 5 and 7 days after initial hemorrhage). Since comprehensive gene expression analyses of the cerebral artery in SAH animal models were performed using mRNA differential display method for the first time [10,11], only a few reports of genome-wide microarray analysis of the cerebral artery in SAH animal models have been published [12-14]. Vikman et al. investigated gene expression changes in rat cerebral arteries 24 hours after SAH and reported that genes related to 'angiogenesis', 'inflammation', and 'extracellular matrix (ECM) remodeling' were differentially expressed [13]. Sasahara et al. investigated dog basilar arteries 7 days after SAH and reported that genes related to 'cell communication', 'host-pathogen interaction', and 'defense immunity protein activity' were upregulated [14]. These two groups investigated only one time point. On the other hand, Macdonald et al. set three time points, days 3, 7, and 14, to first investigate the chronological changes in gene expression in the middle cerebral artery of cynomolgus monkeys [12]. However, the authors investigated only one set of arteries from one animal for each time point. They used the middle cerebral artery that was opposite the clot in the same animals as a control instead of using sham-operated or non-manipulated animals. Although these reports based on a microarray analysis revealed that complex molecular events occurred in the cerebral arteries after SAH, it remains to be elucidated how these complex molecular events change after SAH. Therefore, in the current study, we set four time points (days 0, 3, 5, and 7) and performed microarray analysis to elucidate the overview of alterations in gene expression.

We investigated three animals at each time point (days 0, 3, 5, and 7). Prior to chronological evaluation of the gene expression data obtained with microarray analysis, we confirmed that the gene expression pattern among the three samples at each time point showed a strong positive correlation among samples. Therefore, chronological changes in gene expression and the biological functions revealed in our analysis are likely to show greater reliability than in previous studies.

The present study demonstrated that 1.99% (day 3), 1.38% (day 5), and 1.29% (day 7) of a total of 43,623 genes were differentially expressed after SAH. Sasahara et al. reported that 3.25% of a total of 23,914 genes were differentially expressed in dog basilar artery 7 days after SAH [14]. Macdonald et al. reported that 7.20% of a total of 5,184 genes were differentially expressed during vasospasm [12]. Different species, platforms, control settings, and time point settings among these studies may have lead to this unevenness in DEGs in intra-cranial arteries after SAH. However, these results suggest that fewer than 1,000 genes play an important role in the development of vascular events including cerebral vasospasm after SAH.

After SAH, the number and magnitude of DEGs reached a peak on day 3 and then decreased, whereas the narrowing of the basilar artery reached a peak on day 5 and persisted even on day 7. Comparing the time course of narrowing of the basilar artery with the time course of changes in gene expression, we noted an obvious time lag between the peak of vasospasm and the peak of gene expression following SAH. We previously reported that mRNA expression of endothelin receptor type A is up regulated, with a peak on day 5, whereas protein expression is upregulated with a peak on day 7 after SAH [15]. Schwanhausser et al. reported a strong correlation between mRNA and protein expression levels and that the cellular abundance of proteins is predominantly controlled at the level of mRNA translation [16]. Thus, the time lag between the peak of gene expression and narrowing of the basilar artery after SAH may be caused by the time needed for mRNA translation. In this respect, DEGs with a peak on day 3 may play an important role in the development of cerebral vasospasm, whereas those with a peak on day 5 may play an important role in sustaining cerebral vasospasm. However, what extent those DEGs contribute to cerebral vasospasm still remains to be elucidated.

Gene-related functional categories dynamically changed on day 3

Bioinformatic analysis of DEGs with IPA allows us to understand the dynamic changes that occurred in the cerebral arteries after SAH. Therefore, below, we discuss the gene-related functional categories that were dynamically changed on days 3 and 5.

"Cellular growth and proliferation", "cellular movement" and "cellular development" were the top three functional categories with their highest significant peaks on day 3. The category "cellular growth and proliferation" includes cellular functions such as proliferation, growth, formation, and stimulation (Supplementary Table 1). Smooth muscle cell proliferation in major intra-cranial arteries is considered one of the major pathological changes in spastic arteries after SAH [1]. In mouse cerebral arteries, vascular wall proliferation was initially confirmed 3 hours after SAH and lasted 72 hours after onset [17]. In this functional category, signal transducer and activator of transcription 1 (STAT1) was upregulated in the basilar artery after SAH (Supplementary Table 1). STAT1 has been reported to contribute to arterial wall proliferation during cerebral vasospasm [18].

The category "cellular movement" includes cellular functions such as migration, cell movement, infiltration, and invasion (Supplementary Table 1). After SAH, phenotypic changes in vascular smooth muscle cells (VSMCs) occur, and these cells acquire the ability to migrate, which was confirmed both *in vitro* and *in vivo* [19,20]. Seven days after SAH, phenotypic changes in VSMCs in dog basilar arteries were confirmed with immune histochemical staining for expression of myosin heavy chain subtypes [19]. Tang et al. reported that oxyhemoglobin promotes VSMC migration in 24 hours after oxyhemoglobin exposure [20]. Such dedifferentiated VSMCs may play a pivotal role in sustaining the cerebral vasospasm [19]. Infiltration of inflammatory cells into the media has been reported to represent early morphological changes in cerebral arteries after SAH [1,21,22]. The present study demonstrated that one chemoattractant for monocytes, chemokine C-C motif ligand 2 (CCL2), was upregulated on days 3 and 5 (Supplementary Table 1). This chemotactic chemokine is also known as a putative biomarker of cerebral vasospasm after aneurysmal SAH [23].

The category "cellular development" includes cellular functions such as differentiation, growth, developmental processes, maturation, and development. Two upregulated genes, toll-like receptor 4 (TLR4) and secreted phosphoprotein 1 (SPP1), are included in this category (Supplementary Table 1). TLR4 is activated in the basilar arterial wall during cerebral vasospasm in the rabbit SAH model [24], and inhibition of TLR4 expression by rosiglitazone attenuates cerebral vasospasm in rats [25]. Thus, TLR4 expression and its signaling pathway may participate in the development of cerebral vasospasm. SPP1, also known as osteopontin, is induced in rat brain after SAH [26]. Considering its neuroprotective and pleiotropic effect, SPP1 may have therapeutic potential for treatment of cerebral vasospasm [27,28].

Gene-related functional categories dynamically changed on day 5

The categories "cell-to-cell signaling and interaction", "cell death" and "antigen presentation" were the top three functional categories with their highest significant peaks on day 5.The functional category "cell-to-cell signaling and interaction" includes cellular functions such as activation, binding, adhesion, response, immune response, recruitment, phagocytosis, and stimulation (Supplementary Table 1). Some of these cellular functions overlapped with those of "antigen presentation". Taken together, inflammatory cells and their interactions are activated and participate in the development of cerebral vasospasm as previously reported [1,29]. This functional category includes some inflammatory-related genes that were upregulated after SAH such as C-X-C motif chemokine 10 (CXCL10) and CCL2 (Supplementary Table 1). These results are consistent with the idea of the involvement of inflammation in the development of cerebral vasospasm.

The category "cell death" includes the major two pathways of cell death, apoptosis and necrosis. Apoptosis of endothelial cells and VSMCs in cerebral arteries is considered to play a pivotal role in the pathogenesis of cerebral vasospasm [30,31]. Zubkova et al. reported apoptotic and necrotic findings in both endothelial cells and smooth muscle cells, initially on day 3 [32]. These events progressed over time and were maximal on day 7 in canine basilar artery [32]. These apoptotic changes may cause disruption of the blood-arterial wall barrier in the major cerebral arteries [33,34]. BCL2-related proteinA (BCL2A1), caspase8 (CASP8), and tumor necrosis factor receptor superfamily member 1A (TNFRSF1A) are included in this category (Supplementary Table 1). These findings suggest that several cell death pathways are activated in the arterial wall, causing apoptosis of endothelial cells and VSMCs during vasospasm as previously reported [35,36].

The category "antigen presentation" includes cellular functions such as cell movement, immune response, phagocytosis, recruitment, infiltration, activation, and chemotaxis (Supplementary Table 1). Immune responses against not only autologous blood or damaged tissue but also non-specific immune responses have been considered pathogenesis events in cerebral vasospasm [37,38]. TLR4 was also included in this functional category (Supplementary Table 1). Our result may add further support to the idea of involvement of TLR4 and its signaling pathway in the pathogenesis of cerebral vasospasm.

The present study has two major limitations. First, our study is lack of further confirmation of the microarray results by real-time polymerase chain reaction or western blotting. Further studies are needed to confirm the expression of these molecules that actually play

important roles in the pathogenesis of cerebral vasospasm. Nevertheless, the purpose of the present study is to demonstrate an overview of the chronological changes in gene expressions in the rabbit basilar artery after SAH. Second, the tissue sample of the basilar artery used for the study included not only smooth muscle but endothelium, adventitia, and any inflammatory cells attached to or migrated into the artery. In the present study, it is impossible to confirm the type of cells from which differentially expressed genes derived. Further investigations including in situ hybridization are neededto confirm the origin of differentially expressed genes. However, a large part of DEGs may derive from smooth muscle cells, because smooth muscle cells from the major part of the rabbit basilar arterial wall.

Conclusion

In conclusion, our current study demonstrated chronological changes in gene expression and their biological functions based on annotated ontologies in rabbit basilar arteries after SAH. The number and magnitude of DEGs reached a peak on day 3 and then decreased, whereas narrowing of the basilar artery reached a peak on day 5 and persisted even on day 7. In addition, bioinformatic analysis using IPA revealed that various genes related to "cellular growth and proliferation", "cellular movement" and "cellular development" was dynamically changed in rabbit basilar arteries at the beginning of vasospasm. Genes related to "cell-to-cell signaling and interaction", "cell death" and "antigen presentation" was dynamically changed during the peak of vasospasm. Our findings may provide a simple basis to link the various presumed pathogenesis of vascular events including cerebral vasospasm after SAH based on gene expression analysis.

Acknowledgement

References

1. Kassell NF, Sasaki T, Colohan AR, Nazar G (1985) Cerebral vasospasm following aneurysmal subarachnoid hemorrhage. Stroke 16: 562-572.

2. Stanton LW, Garrard LJ, Damm D, Garrick BL, Lam A, et al. (2000) Altered patterns of gene expression in response to myocardial infarction. Circ Res 86: 939-945.

3. Shi C, Awad IA, Jafari N, Lin S, Du P, et al. (2009) Genomics of human intracranial aneurysm wall. Stroke 40: 1252-1261.

4. Pera J, Korostynski M, Krzyszkowski T, Czopek J, Slowik A, et al. (2010) Gene expression profiles in human ruptured and unruptured intracranial aneurysms: what is the role of inflammation? Stroke 41: 224-231.

5. Bolstad BM, Irizarry RA, Astrand M, Speed TP (2003) A comparison of normalization methods for high density oligonucleotide array data based on variance and bias. Bioinformatics 19: 185-193.

6. Gentleman RC, Carey VJ, Bates DM, Bolstad B, Dettling M, et al. (2004) Bioconductor: open software development for computational biology and bioinformatics. Genome Biol 5: R80.

7. Gentleman R., Carey V, Huber W, Irizarry R, Dudoit S(2005) Bioinformatics and computational biology solutions using R and Bioconductor. Springer, New York.

8. Saeed AI, Sharov V, White J, Li J, Liang W, et al. (2003) TM4: a free, open-source system for microarray data management and analysis. Biotechniques 34: 374-378.

9. Saeed AI, Bhagabati NK, Braisted JC, Liang W, Sharov V, et al. (2006) TM4 microarray software suite. Methods Enzymol 411: 134-193.

10. Onda H, Kasuya H, Takakura K, Hori T, Imaizumi T, et al. (1999) Identification of genes differentially expressed in canine vasospastic cerebral arteries after subarachnoid hemorrhage. J Cereb Blood Flow Metab 19: 1279-1288.

11. Suzuki H, Kanamaru K, Tsunoda H, Inada H, Kuroki M, et al. (1999) Heme oxygenase-1 gene induction as an intrinsic regulation against delayed cerebral vasospasm in rats. J Clin Invest 104: 59-66.

12. Macdonald RL, Zhang ZD, Ono S, Komuro T (2002) Up-regulation of parathyroid hormone receptor in cerebral arteries after subarachnoid hemorrhage in monkeys. Neurosurgery 50: 1083-1091.

13. Vikman P, Beg S, Khurana TS, Hansen-Schwartz J, Edvinsson L (2006) Gene expression and molecular changes in cerebral arteries following subarachnoid hemorrhage in the rat. J Neurosurg 105: 438-444.

14. Sasahara A, Kasuya H, Krischek B, Tajima A, Onda H, et al. (2008) Gene expression in a canine basilar artery vasospasm model: a genome-wide network-based analysis. Neurosurg Rev 31: 283-290.

15. Kikkawa Y, Matsuo S, Kameda K, Hirano M, Nakamizo A, et al. (2012) Mechanisms underlying potentiation of endothelin-1-induced myofilamentCa(2+) sensitization after subarachnoid hemorrhage. J Cereb Blood Flow Metab 32: 341-352.

16. Schwanhausser B, Busse D, Li N, Dittmar G, Schuchhardt J, et al. (2011) Global quantification of mammalian gene expression control. Nature 473: 337-342.

17. Borel CO, McKee A, Parra A, Haglund MM, Solan A, et al. (2003) Possible role for vascular cell proliferation in cerebral vasospasm after subarachnoid hemorrhage. Stroke 34: 427-433.

18. Osuka K, Watanabe Y, Usuda N, Atsuzawa K, Wakabayashi T, et al. (2010) Oxidative stress activates STAT1 in basilar arteries after subarachnoid hemorrhage. Brain Res 1332: 12-19.

19. Yamaguchi-Okada M, Nishizawa S, Koide M, Nonaka Y (2005) Biomechanical and phenotypic changes in the vasospastic canine basilar artery after subarachnoid hemorrhage. J ApplPhysiol (1985) 99: 2045-2052.

20. Tang WH, Zhu G, Zhang JH, Chen Z, Liu Z, et al. (2008) The effect of oxyhemoglobin on the proliferation and migration of cultured vascular smooth muscle cells. ActaNeurochirSuppl (Wien) 104: 197-202.

21. Hughes JT, Schianchi PM (1978) Cerebral artery spasm. A histological study at necropsy of the blood vessels in cases of subarachnoid hemorrhage. J Neurosurg 48: 515-525.

22. Zhang J, Lewis A, Bernanke D, Zubkov A, Clower B (1998) Stroke: anatomy of a catastrophic event. Anat Rec 253: 58-63.

23. Kim GH, Kellner CP, Hahn DK, Desantis BM, Musabbir M, et al. (2008) Monocyte chemoattractant protein-1 predicts outcome and vasospasm following aneurysmal subarachnoid hemorrhage. J Neurosurg 109: 38-43.

24. Zhou ML, Wu W, Ding YS, Zhang FF, Hang CH, et al. (2007) Expression of Toll-like receptor 4 in the basilar artery after experimental subarachnoid hemorrhage in rabbits: a preliminary study. Brain Res 1173: 110-116.

25. Wu Y, Tang K, Huang RQ, Zhuang Z, Cheng HL, et al. (2011) Therapeutic potential of peroxisome proliferator-activated receptor gamma agonist rosiglitazone in cerebral vasospasm after a rat experimental subarachnoid hemorrhage model. J NeurolSci 305: 85-91.

26. Suzuki H, Hasegawa Y, Kanamaru K, Zhang JH (2010) Mechanisms of osteopontin-induced stabilization of blood-brain barrier disruption after subarachnoid hemorrhage in rats. Stroke 41: 1783-1790.

27. Meller R, Stevens SL, Minami M, Cameron JA, King S, et al. (2005) Neuroprotection by osteopontin in stroke. J Cereb Blood Flow Metab 25: 217-225.

28. Xie Y, Sakatsume M, Nishi S, Narita I, Arakawa M, et al. (2001) Expression, roles, receptors, and regulation of osteopontin in the kidney. Kidney Int 60: 1645-1657.

29. Nagata K, Sasaki T, Mori T, Nikaido H, Kobayashi E, et al. (1996) Cisternal talc injection in dog can induce delayed and prolonged arterial constriction resembling cerebral vasospasm morphologically and pharmacologically. SurgNeurol 45: 442-447.

30. Zubkov AY, Ogihara K, Bernanke DH, Parent AD, Zhang JH (2000) Apoptosis of endothelial cells in vessels affected by cerebral vasospasm. SurgNeurol 53: 260-266.

31. Zhou C, Yamaguchi M, Colohan AR, Zhang JH (2005) Role of p53 and apoptosis in cerebral vasospasm after experimental subarachnoid hemorrhage. J Cereb Blood Flow Metab 25: 572-582.

32. Zubkov AY, Tibbs RE, Clower B, Ogihara K, Aoki K, et al. (2002) Morphological changes of cerebral arteries in a canine double hemorrhage model. NeurosciLett 326: 137-141.

33. Sasaki T, Kassell NF, Yamashita M, Fujiwara S, Zuccarello M (1985) Barrier disruption in the major cerebral arteries following experimental subarachnoid hemorrhage. J Neurosurg 63: 433-440.

34. Sasaki T, Kassell NF, Zuccarello M, Nakagomi T, Fujiwara S, et al. (1986) Barrier disruption in the major cerebral arteries during the acute stage after experimental subarachnoid hemorrhage. Neurosurgery 19: 177-184.

35. Cahill J, Calvert JW, Solaroglu I, Zhang JH (2006) Vasospasm and p53-induced apoptosis in an experimental model of subarachnoid hemorrhage. Stroke 37: 1868-1874.

36. Sehba FA, Pluta RM, Zhang JH (2011) Metamorphosis of subarachnoid hemorrhage research: from delayed vasospasm to early brain injury. Mol Neurobiol 43: 27-40.

37. Ostergaard JR, Kristensen BO, Svehag SE, Teisner B, Miletic T (1987) Immune complexes and complement activation following rupture of intracranial saccular aneurysms. J Neurosurg 66: 891-897.

38. Yanamoto H, Kikuchi H, Okamoto S, Nozaki K (1994) Cerebral vasospasm caused by cisternal injection of polystyrene latex beads in rabbits is inhibited by a serine protease inhibitor. SurgNeurol 42: 374-381.